IOP Conf. Series: Materials Science and Engineering **377** (2018) 012023 doi:10.1088/1757-899X/377/1/012023

Effect of Mn on corrosion and thermal behaviour of $AlCr_{1.5}CuFeNi_2Mn_x$ high-entropy alloys

V kukshal[1], A Patnaik[2] and I K Bhat[3]

[1]Assistant Professor, Mechanical Engineering Department, NIT, Uttarakhand-246174, India
[2]Assistant Professor, Mechanical Engineering Department, MNIT Jaipur-302017, India
[3]Professor, Applied Mechanics Department, MNNIT Allahabad-211004, India

E-mail: vikaskukshal@nituk.ac.in

Abstract. There are numerous multicomponent alloys reported in the past resulting in a single phase with promising mechanical properties at high temperature. However, investigation on the corrosion properties and thermal conductivity of the novel high-entropy alloy (HEAs) are yet to be explored. The present study focuses on the effect of Mn on the corrosion and thermal behaviour of $AlCr_{1.5}CuFeNi_2Mn_x$ (x = 0, 0.25, 0.5, 0.75,1 in molar ratio) HEAs. The HEAs reported so far are mostly fabricated by arc melting process whereas, in this study, $AlCr_{1.5}CuFeNi_2Mn_x$ HEAs ingots were cast by high temperature vacuum induction furnace under inert gas environment. The electrochemical-corrosion behaviour of the as-cast alloys was studied using a potentiodynamic-polarization method immersed in 3.5 wt. %NaCl solution (open to air) at room temperature. It was observed from the polarization curve that the corrosion resistance was found to increase on the addition of higher amount of Mn in base alloy. The thermal conductivity of the HEAs was determined at 300 K, 350 K, 400 K, 450 K and 500 K. It was found that the thermal conductivity of the alloys decreases with the addition of the Mn content whereas the thermal conductivity is found to increase with the increase in the temperature of the alloys.

1. Introduction

Materials have undergone continuous evolution from the use of single elements to alloys and in recent year's multi-component alloys called high-entropy alloys (HEAs). High-entropy alloys consist of at least five principle elements in either equimolar or near-equimolar ratio. The atomic percentage of each element varies from 5-35 at. % [1-2]. The high-entropy alloy show excellent improvement in properties such as high hardness [3-4], high tensile strength [5-6], high compressive strength [7-8], wear resistance [9-10] and excellent corrosion resistance [11-14]. These properties are due to the high configurational entropy of the HEAs as compared to the conventional alloys thus exhibiting solid-solution structures. Their distinctive properties make them suitable for various applications such as: thermal and wear and resistant coatings, components for nuclear power plants, structural materials for transportation and energy industries and so on. In most of these applications, the high-temperature oxidation behaviour and thermal stability are amongst the most important criteria.

The most of the studies are based on the equimolar or near equimolar high-entropy alloy system consisting of Al (FCC), Fe (BCC), Cr (BCC), Cu (FCC) and Ni (FCC) resulting in mixed FCC and BCC phase [15-18]. The hardness of the $Al_xCrCuFeNi_2$ (x = 0.2–2.5) alloys increased to the large extent on the addition of Aluminium and the phase changed from FCC to BCC + ordered BCC phase [15]. Another study based on $AlCrCuFeNi_2$ reveals that the dynamic yield strength approximately shows a linear relationship with the strain rate and the strain hardening rate is significantly enhanced by dynamic loading specially at the initial plastic stage [16]. Microstructural examination of the as-cast $AlCrCuFeNi_2$ alloy shows typical dendrite (DR) and interdendrite (ID) structures and on heating

at 600 °C, the DR region remains Cr-Fe-Ni rich phase whereas some spherical precipitates changed to the needle-like structure within the ID regions [18].

The study of oxidation behaviour of the novel HEAs is very important keeping in view the various high temperature applications of materials resulting in the severe oxidation. Hsu et al. studied the corrosion performance of $FeCoNiCrCu_x$ high-entropy alloys and reported that the addition of copper content in the alloy increases the affinity to localized corrosion due to the formation of Cu-rich inter-dendrite and Cu-depleted dendrite [19]. Lee et al. studied the effect of Aluminium (x=0, 0.3, 0.5) addition on $Al_xCrFe_{1.5}MnNi_{0.5}$ alloys and found that the corrosion resistance values increases from 21 to 34 Ωcm^2 as the aluminum content increased from 0 to 0.5 mol in 0.1 M HCl solution, and were evidently less than 304 stainless steel ($243\Omega cm^2$) [20].Chou et al. investigated the electrochemical properties of the $Co_{1.5}CrFeNi_{1.5}Ti_{0.5}Mo_x$ HEAs and established that the Mo alloys are not prone to pitting corrosion in the presence of NaCl solution [21].Various studies are also based on investigating the effect of elements on the thermal conductivity of the HEAs. Chou et al. found that the thermal conductivity of $Al_xCoCrFeNi$ alloys increases with increasing temperature [22]. The thermal conductivity of series of CoCrFeNi, AlCoCrFeNi, $Al_2CoCrFeNi$HEAs was found to be 12, 11 and 16 W/mK [23].

From the above literature, it can be stated that the study of corrosion behaviour and thermal conductivity of novel HEAs is yet to be explored in order to meet the particular application such as in case of the heat exchanger where these properties of material play a very important role. The aim of this study is to investigate the influence of Mn content on the corrosion and thermal behaviour of $AlCr_{1.5}CuFeNi_2Mn_x$ (where x= x = 0, 0.25, 0.5, 0.75,1 in molar ratio) high-entropy alloys in the ambient atmosphere.

2. Materials and methods

HEAs ingots with composition of $AlCr_{1.5}CuFeNi_2Mn_x$ (x = 0, 0.25, 0.5, 0.75,1 in molar ratio) were prepared using high temperature vacuum induction furnace under inert gas environment. The elements Al, Cr, Cu, Fe, Ni and Mn were used as raw material in the form of the solid granules with purity above 99.9%. Approximately 800 g of raw materials were melted in a water-cooled chamber containing ceramic crucible under the argon atmosphere to prevent oxidation. The melting was repeated five times with electromagnetic stirring to improve the chemical homogeneity.

Table1. Energy Dispersive X-ray Spectroscopy (EDS) analysis of $AlCr_{1.5}CuFeNi_2$ high- entropy alloy

Composition	Al	Cr	Cu	Fe	Ni
at.%	13.26	22.93	15.01	15.07	33.73
wt.%	6.72	22.39	17.91	15.80	37.18

The dimensions of the produced ingots were about 140 mm × 90 mm × 10 mm. Table 1 shows the amount (g) of metals available in the produced HEAs as determined by EDS. The chemical composition of $AlCr_{1.5}CuFeNi_2$ alloy as measured by EDS analysis is close to its original composition.

The electrochemical corrosion test was performed on a sample of size 10 mm × 10 mm by potentiodynamic-polarization measurement using 3.5 wt.% NaCl solution at room temperature. An electrochemical workstation (GAMRY Reference 600TM) was used for corrosion test with measurements recorded at a scan rate of 0.5 mVs^{-1} in the range of -1 to 0.5 V.The electrochemical impedance spectra were attained at the open circuit potential in the frequency range of $10^5 – 10^{-2}$ Hz to 0.01 Hz with the amplitude of 5 mV.All the samples were dipped in NaCl solution for one and half

hour before the test, allowing the system to reach equilibrium with the electrolyte exposing the sample to an area of 1 cm^2 to the solution. The corrosion rates for each alloy can be calculated using the following expression

$$K_{corr} = \frac{i_{corr}\ K.\ EW}{\rho}$$

where: i_{corr} = Corrosion current density (A cm^{-2})
ρ = mass density (g cm^{-3}),
EW= Equivalent weight of the electrode (g),
k (constant) = 3272 mm/(A-cm-year)),
K_{corr}= Corrosion rate in millimetres per year (mmpy).

The thermal conductivity of alloys was measured by hot disk method using thermal constant analyzer (Hot Disk TPS 500, Gothenburg, Sweden). A sample of dimension 25 mm × 25 mm with 10 mm thickness was used for conducting the experiment. The thermal conductivity of the samples was measured at various temperatures ranging from 300 K to 500 K at a step size of 50 K.

3. Results and discussion

3.1 *Electrochemical corrosion properties*

Polarization curves of the $AlCr_{1.5}CuFeNi_2Mn_x$ high-entropy alloys are shown in Fig. 1 and their electrochemical parameters are listed in Table 2.The results indicate that the corrosion resistance of the HEAs is improving with the addition of Mn content. The polarization curve indicates that as the Mn content increases from $Mn_{0.25}$ to Mn, HEAs almost overlap each other signifying that the alloys are almost alike in corrosion resistance behaviour. Fig. 1 shows an initial increase in the corrosion rate from x = 0 to x = 0.5 and further decreases with increase in the Mn content. The HEAs with larger corrosion potential (E_{corr}) and smaller corrosion current density (i_{corr}) have better corrosion resistance. E_{pit} is the potential value where the current is suddenly increased, which means the HEAs start to pit. The improvement in the corrosion resistance of the HEAs is due to the proper distribution of the Ni and Cr in the solid solution due to the addition of the Mn content. On the contrary, the addition of Mn in $Al_{0.3}CoCrFeNiMn_x$ slightly decreases the corrosion resistance of the alloy [24].

Table 2. Electrochemical parameters of Mn_0, $Mn_{0.25}$, $Mn_{0.5}$, $Mn_{0.75}$ and Mn alloys from potentiodynamic- polarization curve.

High-entropy alloy	Designation	E_{corr}(mV)	I_{corr} (μA/cm^2)	E_p(V)	Corrosion rate (mpy)
$AlCr_{1.5}CuFeNi_2Mn_0$	Mn_0	-727.6	7.327	-0.7252	2.172
$AlCr_{1.5}CuFeNi_2Mn_{0.25}$	$Mn_{0.25}$	-437.5	11.56	-0.4346	4.040
$AlCr_{1.5}CuFeNi_2Mn_{0.5}$	$Mn_{0.5}$	-435.1	27.04	-0.4346	9.531
$AlCr_{1.5}CuFeNi_2Mn_{0.75}$	$Mn_{0.75}$	-354.0	17.13	-0.3475	6.093
$AlCr_{1.5}CuFeNi_2Mn$	Mn	-383.4	9.888	-0.3814	3.574

3.2 *Thermal conductivity*

This part of the study investigates the thermal behaviour of $AlCr_{1.5}CuFeNi_2Mn_x$ HEAs. Thermal conductivity k(T) is a measure of thermal diffusion coefficient α (T), density ρ (T) and specific heat s (T) of the material at temperature T [25]. Fig. 2(a) shows the graph between thermal conductivity and molar ratio x in $AlCr_{1.5}CuFeNi_2Mn_x$ HEAs. It is found that the thermal conductivity of the HEAs decreases with increase in the value of x. This is due to the dual phase FCC+BCC present in the HEAs. The phenomenon can be explained with respect to the larger scattering effect due to the addition of the Mn content and hence decrease in the thermal conductivity. The duplex phase is characterised by the more interface boundary as compared to the single phase resulting in the lowering of the heat transfer in the HEAs. Chou et al. found the similar observation while studying the thermal conductivity of $Al_xCoCrFeNi$ [25].

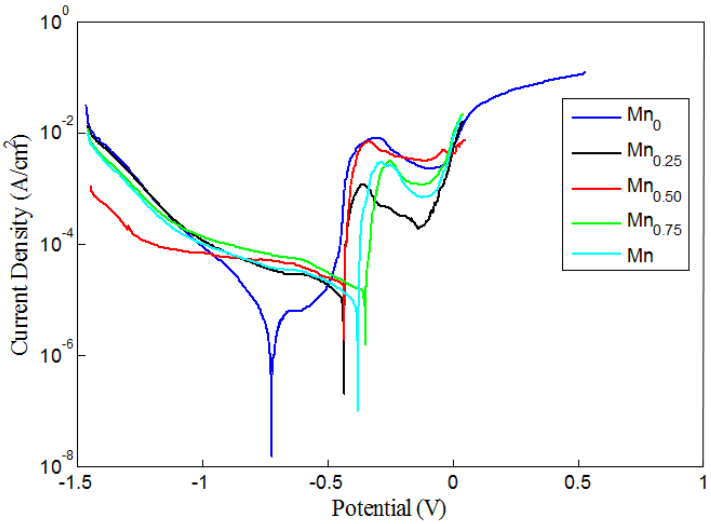

Figure 1: Potentiodynamic-polarization curves of $AlCr_{1.5}CuFeNi_2Mn_x$ HEAs in 3.5 wt. % NaCl at ambient temperature.

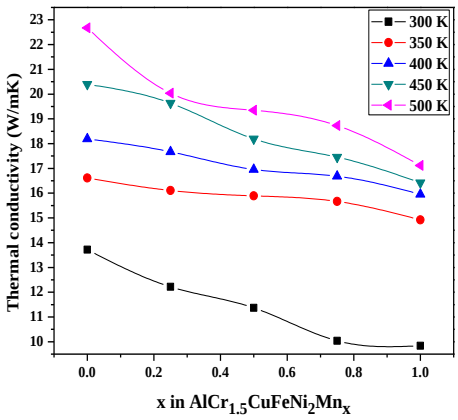

Figure 2(a): Variation of thermal conductivity as a function of x in $AlCr_{1.5}CuFeNi_2Mn_x$.

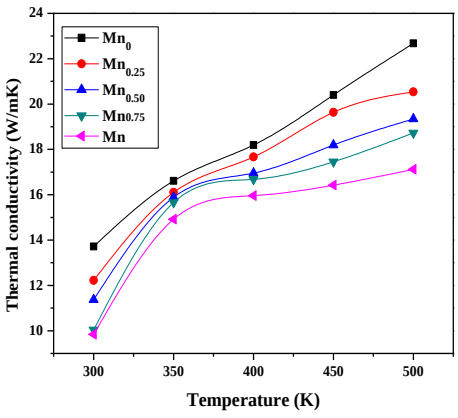

Figure 2(b): Variation of thermal conductivity as a function of temperature.

Fig. 2(b) shows the variation of thermal conductivity of alloys as a function of temperature. Due to small carrier concentration in the lower range of temperatures along with the low sensitivity of the photon concentration, the thermal conductivity of the HEAs increases at higher temperatures. In addition to that, the mean free path of electrons increases with temperature due to the large linear thermal expansion in the HEAs resulting in the higher thermal conductivity with respect to the increase in the temperature.

4. Conclusions

Based on the above investigations, the following concluding remarks are listed from the study:

1. The $AlCr_{1.5}CuFeNi_2Mn_x$ HEAs was successfully fabricated by the high vacuum induction casting machine resulting in the dual phase FCC+BCC.
2. The corrosion resistance of $AlCr_{1.5}CuFeNi_2Mn_x$ HEAs first decreases and then increases with the addition of Mn content at room temperature in 3.5wt.% NaCl solution. The high amount of Mn addition facilitates the formation of solid solution resulting in the increase in the corrosion resistance.
3. The thermal conductivity of $AlCr_{1.5}CuFeNi_2Mn_x$ decreases with the increase in the molar ratio of Mn whereas the thermal conductivity of the HEAs is found to increase with the increase in the temperature. The duplex phase results in the smaller value of thermal conductivity due to the more barriers in the path of the carriers.

References

[1] Yeh J W, Chen S K, Lin S J, Gan J Y, Chin T S, Shun T T, Tsau C H and Chang S Y 2004 *Adv. Eng. Mater.***6** 99-303.
[2] Huang P K, Yeh J W, Shun T T and Chen S K *Adv. Eng. Mater.* 2004 **6** 74-8.
[3] Huang Y S, Chen L, Lui H W, Cai M H and Yeh J W 2007 *Mater. Sci. Eng. A.* **457(1)** 77-83.
[4] Hsieh K C, Yu C F, Hsieh W T, Chiang W R, Ku J S, Lai J H, Tu C P and Yang C C 2009 *J. Alloys Compd.* ***483*****(1)**, 209-2
[5] Gaganov A, Freudenberger J, Botcharova E and Schultz L 2006 *Mater. Sci. Eng. A.* **437(2)** 313-22.
[6] Otto F, Dlouhy A, Somsen C, Bei H, Eggeler G and George E P 2013 *Acta Mater.* **61(15)** 743-55.
[7] Zhou Y J, Zhang Y, Wang Y L and Chen G L 2007 *Mater. Sci. Eng. A.* **454** 260-5.
[8] Wang Y P, Li B S, Ren M X, Yang C and Fu H Z 2008 *Mater. Sci. Eng. A.* **491(1)** 154-8.
[9] Wu J M, Lin S J, Yeh J W, Chen S K, Huang Y S and Chen H C 2006 *Wear.* **261(5)** 513-9.
[10] Chuang M H, Tsai M H, Wang W R, Lin S J and Yeh J W 2011 *Acta Mater.* **59 (16)** 6308-17.
[11] Zhang S, Wu C L, Zhang C H, Guan M and Tan J Z 2016 *Opt. Laser Technol.* **84** 23-31.
[12] Zhang Z, Axinte E, Ge W, Shang C and Wang Y 2016 *Mater. Des.* **108** 106-13.
[13] Dąbrowa J, Cieślak G, Stygar M, Mroczka K, Berent K, Kulik T and Danielewski M 2017 *Intermetallics* **84** 52-61.
[14] Ye Q, Feng K, Li Z, Lu F, Li R, Huang J and Wu Y 2017 *Appl. Surf. Sci.* **396** 1420-6.
[15] Guo S, Ng C and Liu C T 2013 *J. Alloys Compd.* **557** 77-81.
[16] Ma S G, Jiao Z M, Qiao J W, Yang H J, Zhang Y and Wang Z H 2016 *Mater. Sci. Eng. A.* **649** 35-8.
[17] Wang Z, Li J, Fang Q, Liu B and Zhang L 2017 *Appl. Surf. Sci.* **416** 470-81.
[18] Guo L, Wu W, Ni S, Wang Z and Song M 2017 *Micron.***101** 69-77.

[19] Hsu Y J, Chiang W C and Wu J K 2005 *Mater. Chem. Phys.* **92** 112–7.
[20] Lee C P, Chen Y Y, Hsu C Y, Yeh J W and Shih H C 2008 *Thin Solid Films* **517**1301–1305.
[21] Chou Y L, Yeh J W and Shih H C 2010 *Corros. Sci.* **52**2571–81.
[22] Chou H P, Chang Y S, Chen S K and Yeh J W 2009 *Mater. Sci. Eng. B.* **163(3)** 184-9.
[23] Tsai M H 2013 *Entropy.* **15(12)** 5338-45
[24] Wong S K, Shun T T, Chang C H and Lee C F 2017 *Mater. Chem. Phys.* **xxx** 1-6.
[25] Chou H P, Chang Y S, Chen S K and Yeh J W 2009 *Mater. Sci. Eng. B.* **163** 184–9.